PHYSICAL REVIEW A **82**, 021605(R) (2010)

Temperature and coupling dependence of the universal contact intensity for an ultracold Fermi gas

F. Palestini, A. Perali, P. Pieri, and G. C. Strinati
Dipartimento di Fisica, Università di Camerino, I-62032 Camerino, Italy

(Received 6 May 2010; revised manuscript received 24 June 2010; published 23 August 2010)

Physical properties of an ultracold Fermi gas in the temperature-coupling phase diagram can be characterized by the contact intensity C, which enters the pair-correlation function at short distances and describes how the two-body problem merges into its surrounding. We show that the local order established by pairing fluctuations about the critical temperature T_c of the superfluid transition considerably enhances the contact C in a temperature range where pseudogap phenomena are maximal. Our *ab initio* results for C in a trap compare well with recently available experimental data over a wide coupling range. An analysis is also provided for the effects of trap averaging on C.

DOI: 10.1103/PhysRevA.82.021605 PACS number(s): 03.75.Ss, 03.75.Hh, 74.40.−n, 74.20.−z

The "contact" C, introduced by Tan [1,2] to characterize the merging of two-body into many-body physics in systems like ultracold Fermi gases with a short-range interparticle interaction, has attracted much interest lately [3–7]. This is especially relevant in the context of the BCS-BEC crossover, whereby a smooth evolution occurs jointly for the two-body and many-body physics, from the presence of Cooper pairs with an underlying Fermi surface in the BCS limit, to the formation of molecular bosons with a residual interaction in the Bose-Einstein condensate (BEC) limit.

Recently, the contact C was measured in an ultracold gas of trapped fermionic (^{40}K) atoms [8], from the large-momentum tail of the momentum distribution as well as from the high-frequency tail of the radio-frequency signal following an earlier suggestion [9]. These measurements were done from about unitarity (where the scattering length a_F of the Fano-Feshbach resonance diverges) to deep inside the BCS region [more precisely, in the coupling range $-2.5 \lesssim (k_F a_F)^{-1} \lesssim +0.5$ where $k_F = (2mE_F)^{1/2}$ is the Fermi wave vector expressed in terms of the Fermi energy $E_F = \omega_0(3N)^{1/3}$, m being the atom mass, N the total number of atoms, and ω_0 the average trap frequency [10]], and in a temperature range about the critical temperature T_c.

Several questions concerning the contact C remain open. They hinge on the recent experimental results of Ref. [8] (like the temperature and coupling dependence of C, and the effect that trap averaging has on the values of C), as well as on more theoretical issues. These include the identification of the (approximate) spatial boundary between short-range and medium-range physics that can be associated with the contact C, the effects that improved theoretical approaches have on the values of C, and the interconnection with the presence of a pseudogap in the single-particle excitation spectrum.

In this paper, we address these questions and calculate the contact C using a t-matrix approach [11] that proved successful in comparison with data obtained from momentum-resolved radiofrequency spectroscopy to realize an analogue of photoemission spectroscopy for ultracold Fermi atoms [12], and also using a nontrivial extension of this theory [13] which takes into account the residual interaction among composite bosons. This is to verify to what an extent improvements on the description of the medium-range physics (over and above the results of the t matrix) influence the values of C in different coupling and temperature ranges [14].

We shall, specifically, be concerned with the temperature dependence of C over an *extended* temperature range up to (several times) the Fermi temperature T_F to determine how the value of C is affected by the pseudogap physics extending above T_c in the unitary $[-1 \lesssim (k_F a_F)^{-1} \lesssim +1]$ regime, and to address the related question of how trap averaging influences the value of C with respect to that of a homogeneous system with the same nominal temperature and coupling.

The contact C was originally introduced to account for the large wave-vector behavior of the fermionic distribution $n(k)$ (for spin component) of the homogeneous system, such that $n(k) \approx C_h\, k^{-4}$. Here the suffix "$h$" stands for homogeneous, $k = |\mathbf{k}|$ is in units of $k_F = (3\pi^2 n)^{1/3}$ where n is the total particle density, and $n(k)$ is normalized such that $\int \frac{d\mathbf{k}}{(2\pi)^3}\, n(k) = 1/2$. Alternatively, C_h can be extracted from the high-frequency tail of the radio-frequency (rf) spectrum $I_{\rm rf}(\omega)$ per unit volume, so that $I_{\rm rf}(\omega) \approx (C_h/2^{3/2}\pi^2)\, \omega^{-3/2}$. Here the frequency ω is in units of E_F and the rf spectrum is normalized such that $\int_{-\infty}^{+\infty} d\omega\, I_{\rm rf}(\omega) = 1/2$. The above asymptotic form of $I_{\rm rf}(\omega)$ holds provided final-state effects can be neglected [9,15,16].

Similar asymptotic behaviors can be obtained for the trapped system. Preserving the above normalization as for the homogeneous system, we write within a local-density approximation

$$n(k) = \int d\mathbf{r}\, n(k;\mathbf{r}) \approx \frac{C_t}{k^4}, \tag{1}$$

where

$$C_t = \frac{8}{\pi^2} \int d\mathbf{r}\, \frac{[3\pi^2\, n(\mathbf{r})]^{4/3}}{k_F^4}\, C_h(\mathbf{r}). \tag{2}$$

Here the suffix "t" and k_F refer to the trapped system, the spatial position $\mathbf{r}$ is in units of the Thomas-Fermi radius $R_F = [2E_F/(m\omega_0^2)]^{1/2}$, and $n(\mathbf{r})$ and $C_h(\mathbf{r})$ are the density and contact *locally* in the trap. By a similar token, the large-ω behavior of the total rf spectrum of the trapped system reduces to

$$I_{\rm rf}(\omega) = \int d\mathbf{r}\, I_{\rm rf}(\omega;\mathbf{r}) \approx \frac{C_t}{2^{3/2}\pi^2\, \omega^{3/2}}, \tag{3}$$

with the overall normalization of the homogeneous case.

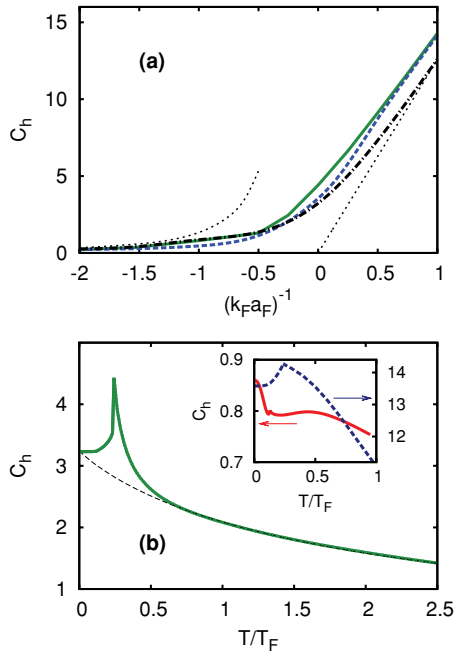

FIG. 1. (Color online) The contact C_h for the homogeneous case: (a) At T_c vs the coupling $(k_F a_F)^{-1}$, obtained within the t-matrix approximation (full line) and its improved Popov version (dashed line). The leading approximations in weak and strong coupling (light-dotted lines) as well as the $T = 0$ result within the t-matrix approximation (dashed-dotted line) are also reported. (b) At unitarity vs T/T_F, obtained within the t-matrix (full line). The high-temperature approximation to this curve is also reported as a reference (dashed line) and extrapolated to $T = 0$. [See the text for the meaning of the inset.]

This local-density analysis shows that, by adding contributions of different shells with a weight proportional to $n(\mathbf{r})^{4/3}$, the trap modifies the value C_h for a homogeneous system at the same nominal coupling $(k_F a_F)^{-1}$ and (relative) temperature T/T_F. In this respect, the temperature dependence of C_h provides important information because different shells are at different relative temperature with respect to the local value of T_F.

We begin our analysis with the homogeneous case at T_c and show in Fig. 1(a) the coupling dependence of C_h, when $n(k)$ is obtained within the t-matrix approximation of Ref. [11] (full line) and its improved Popov version of Ref. [13] (dashed line). The calculations are done at the value of T_c of the respective theories. The plot also shows (light-dotted lines) the leading (low-temperature) approximations for C_h obtained in the BCS weak-coupling and BEC strong-coupling limits, which are given by the expressions $(4/3)k_F^2 a_F^2$ and $4\pi/(k_F a_F)$, respectively, with the crossover region $-1 \lesssim (k_F a_F)^{-1} \lesssim +1$ marking the change between these two limiting behaviors.

Note how the difference between the full and dashed lines in Fig. 1(a), which originates from the activation of the residual interaction among the composite bosons, is appreciable only close to unitarity where particles correlate with each other within the interparticle spacing k_F^{-1}. The smallness of this difference resulting from our calculations confirms the validity of the t-matrix approximation for the contact C_h and for the high-energy scale to which C_h is associated. Yet this difference is relevant for the physical interpretation of the contact C_h as characterizing the effects of medium-range (many-body) physics over and above the short-range (two-body) physics. This interpretation is also consistent with rewriting $C_h = (3\pi^2/4)(\Delta_\infty/E_F)^2$ in terms of the high-energy scale Δ_∞ introduced in Ref. [9], such that $\Delta_\infty = 2\pi|a_F|n/m$ embodies in weak coupling the effects of surrounding particles through a mean-field shift [17], while $\Delta_\infty^2 = 4\pi n/(m^2 a_F)$ reflects a standard relation in strong coupling [18] between the density and the gap parameter within BCS theory. For comparison, Fig. 1(a) also reports the coupling dependence of C_h at zero temperature (dashed-dotted line) within the t-matrix approximation, to which the above approximate expressions in the BCS and BEC limits converge. This dependence is in agreement with that obtained in Ref. [19] within a Gaussian pair-fluctuation theory.

Figure 1(b) shows the temperature dependence of C_h at unitarity over an extended temperature range within the t-matrix approximation. The rather slow decay of C_h at high temperature is consistent with the expectation that C_h is not related to long-range order. The temperature behavior of C_h steepens up at low temperature when entering the pseudogap region for $T/T_F \lesssim 0.5$ [12], thus evidencing the emergence of a local (medium-range) order which is also responsible for the pseudogap. Such an enhancement of the value of C_h appears most evident when the calculation is continued below T_c [20], with the result that a cusp appears in C_h at T_c where the effect of the pseudogap is maximum. To emphasize this enhancement, we have indicated in Fig. 1(b) the extrapolation of the high-temperature behavior of C_h (dashed line) down to $T = 0$, on top of which the contribution associated with the pseudogap region about T_c appears evident. Our value (=3.23) for C_h at $T = 0$ compares well with that (=3.40) extracted from the Monte-Carlo calculations of Ref. [21]. For completeness, the inset of Fig. 1(b) reports the temperature dependence of C_h for $(k_F a_F)^{-1} = -1.0$ (full line, left scale) and $(k_F a_F)^{-1} = +1.0$ (dashed line, right scale). The maximum at $T/T_F \simeq 0.5$ in the weak-coupling curve is consistent with the Fermi-liquid behavior discussed in Ref. [14].

The temperature dependence of C_h is here reported for the first time and deserves further comments. On physical grounds, the enhancement of C_h when entering the fluctuative region above T_c is due to the strengthening of local pairing correlations in the absence of long-range order. In this respect, the most appealing definition of the contact is through the short-range behavior of the pair-correlation function between opposite spins [1]. This quantity is affected by pairing fluctuations in the particle-particle channel, of which the t-matrix represents the most important contribution. In addition, the contact C_h, through its alternative definition in terms of the high-energy scale Δ_∞ that was previously mentioned, can be related to a wave vector and frequency averaging of the pair-fluctuation propagator [9]. The wave-vector and frequency structures of the very same pair-fluctuation propagator also give rise to a characteristic low-energy scale Δ_{pg} in the single-particle excitations [11], which is referred to as the pseudogap. The interdependence between the two energy scales Δ_∞ and Δ_{pg} can then be explicitly appreciated in Fig. 2, where they are shown at T_c versus the coupling

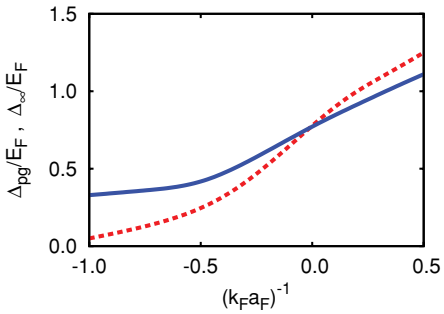

FIG. 2. (Color online) The high-energy scale Δ_∞ (full line) and the low-energy scale Δ_{pg} (dashed line) are reported (normalized to E_F) vs the coupling $(k_F a_F)^{-1}$ at T_c.

$(k_F a_F)^{-1}$. The two energy scales do not fully relate to each other in weak coupling where the contact is dominated by the mean-field interaction, but become very close in value at unitarity where strong local-pairing correlations dominate both thermodynamic (Δ_∞) and dynamic (Δ_{pg}) quantities.

Although the values of C_h are extracted from the asymptotic (scale-free) power law $n(k) \approx C_h\, k^{-4}$, a characteristic value k_C can nevertheless be identified at which $n(k)$ has reached $C_h\, k^{-4}$ within, say, a few percent accuracy. The length scale corresponding to k_C^{-1} is approximately the spatial range at which two-body physics interfaces with medium-range physics. This range is expected to be about the size of the composite bosons in strong coupling and the interparticle spacing in weak coupling. Figure 3 shows the values of k_C extracted in this way at T_c versus $(k_F a_F)^{-1}$ within the t-matrix approximation, for the three distinct values (2.5,5,10)% of the above percent accuracy. In extreme weak coupling, our numerical values recover the limiting ones obtained for a dilute Fermi gas [22]. Note how k_C reaches a pronounced minimum for the coupling at which the chemical potential vanishes, away from which k_C increases most markedly on the strong-coupling side as expected from the increasing spatial localization of composite bosons.

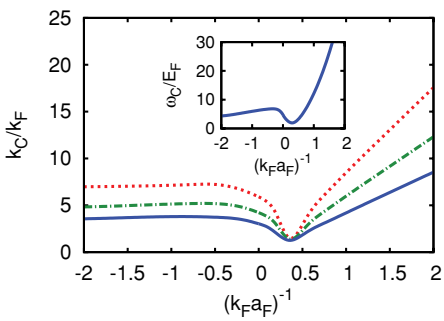

FIG. 3. (Color online) The characteristic values of k_C (normalized to k_F), at which the asymptotic power-law behavior $n(k) \approx C_h\, k^{-4}$ is reached within 2.5% (dashed line), 5% (dashed-dotted line), and 10% (full line) accuracy, are shown at T_c versus $(k_F a_F)^{-1}$. The inset shows, correspondingly, the characteristic value ω_C (normalized to E_F), at which the asymptotic power-law behavior $I_{rf}(\omega) \approx (C_h/2^{3/2}\pi^2)\,\omega^{-3/2}$ of the rf spectrum is reached within 10% accuracy.

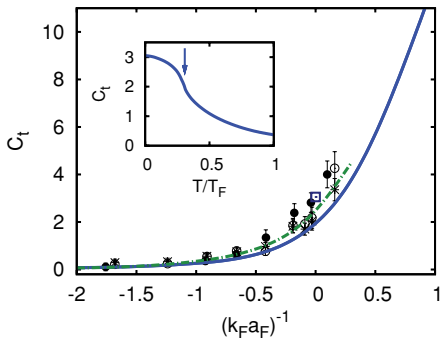

FIG. 4. (Color online) The contact C_t obtained within the t-matrix approximation for the trapped case (full line) is shown at T_c vs the coupling $(k_F a_F)^{-1}$, and compared with the experimental values of Ref. [8] (filled and empty circles, stars). The inset shows, correspondingly, C_t at unitarity vs T/T_F.

In addition, the inset of Fig. 3 shows the value of ω_C at T_c versus $(k_F a_F)^{-1}$, extracted within a 10% accuracy from the large-ω behavior of the rf spectrum. (Recall that the $\omega^{-3/2}$ tail of the rf spectrum originates from the short-range behavior of the two-body wave function [23,24] in the absence of final-state effects [25].) A comparison with k_C with the same accuracy yields the relation $2\omega_C = k_C^2$ that holds approximately for all couplings.

The values of the contact C_t obtained from Eq. (1), by adding the asymptotic contributions from all shells in the trap within the t-matrix approximation, are reported in Fig. 4 at T_c versus $(k_F a_F)^{-1}$ (full line). They are compared with the values (filled and empty circles, stars) obtained experimentally in Ref. [8] through alternative procedures. Note that in the experiment the system is above (below) T_c in the BCS (BEC) side of the unitary region. The theoretical value obtained at unitarity for $T = 0$ is also reported for comparison (empty square). Due to difficulties in extracting the asymptotic behavior of $n(k)$ from experimental data, the figure also shows the theoretical values of C_t (dashed-dotted line) obtained upon averaging $k^4 n(k)$ over the interval $k_{min} \leqslant k \leqslant k_{max}$. This follows the procedure used to extract the experimental values of C_t, for which $k_{min} = 1.55$ when $(k_F a_F)^{-1} < -0.5$ and $k_{min} = 1.85$ when $-0.5 < (k_F a_F)^{-1}$, while $k_{max} = 2.5$ [8].

It is worth noting that the data of Ref. [8] which are reported in Fig. 4, have been originally compared with a theoretical curve from Ref. [4], where the behavior of C_t at $T = 0$ was obtained across the unitary regime by interpolating known results in the BCS and BEC limits. That interpolation has to be contrasted with the completely *ab initio* theoretical calculation at T_c reported by the full line in Fig. 4, which spans a wide coupling range just across the unitary regime. A similar calculation at $T = 0$ within a Gaussian pair-fluctuation theory has been reported in Ref. [19].

Finally, the inset of Fig. 4 displays the temperature dependence of C_t for the trapped case at unitarity within the t-matrix approximation (full line), with the vertical arrow indicating the corresponding value of T_c. Contrary to the result for the homogeneous case of Fig. 1(b), no cusp now appears in C_t at T_c for the trapped case. An expanded discussion about the effects that trap averaging has on the values of C is provided

in [26]. In addition, we note that for $T \gtrsim T_F$ we retrieve the $T^{-5/2}$ dependence reported in Ref. [27], while for $T \lesssim T_F$ our results somewhat differ from the (high-temperature) virial expansion of Ref. [19].

In conclusion, we have presented a detailed analysis of the contact intensity C for a Fermi gas over the temperature-coupling phase diagram. The values of C have been obtained from the large-k behavior of the momentum distribution $n(k)$ as well as from the large-ω tail of the rf spectrum $I_{\rm rf}(\omega)$, both for the homogeneous and trapped case. For the latter case, good agreement is obtained with recent experimental data. The effects of pairing fluctuations on C have been determined by the t-matrix approximation and its improved Popov version that takes into account the interaction among composite bosons. We have found that the values of C are strongly affected by the emergence of a pseudogap in the single-particle excitations about T_c.

ACKNOWLEDGMENTS

Discussions with E. Cornell, D. Jin, and J. T. Stewart are gratefully acknowledged. This work was partially supported by the Italian MIUR under Contract No. PRIN-2007 "Ultracold Atoms and Novel Quantum Phases."

[1] S. Tan, Ann. Phys. (NY) **323**, 2952 (2008).
[2] S. Tan, Ann. Phys. (NY) **323**, 2971 (2008).
[3] E. Braaten and L. Platter, Phys. Rev. Lett. **100**, 205301 (2008).
[4] F. Werner, L. Tarruell, and Y. Castin, Eur. Phys. J. B **68**, 401 (2009).
[5] S. Zhang and A. J. Leggett, Phys. Rev. A **79**, 023601 (2009).
[6] R. Combescot, F. Alzetto, and X. Leyronas, Phys. Rev. A **79**, 053640 (2009).
[7] F. Werner and Y. Castin, e-print arXiv:1001.0774v1.
[8] J. T. Stewart, J. P. Gaebler, T. E. Drake, and D. S. Jin, Phys. Rev. Lett. **104**, 235301 (2010).
[9] P. Pieri, A. Perali, and G. C. Strinati, Nature Phys. **5**, 736 (2009).
[10] We set $\hbar = 1$ and $k_B = 1$ throughout.
[11] A. Perali, P. Pieri, G. C. Strinati, and C. Castellani, Phys. Rev. B **66**, 024510 (2002).
[12] J. P. Gaebler, J. T. Stewart, T. E. Drake, D. S. Jin, A. Perali, P. Pieri, and G. C. Strinati, Nature Phys. **6**, 569 (2010).
[13] P. Pieri and G. C. Strinati, Phys. Rev. B **71**, 094520 (2005).
[14] Z. Yu, G. M. Bruun, and G. Baym, Phys. Rev. **80**, 023615 (2009).
[15] W. Schneider and M. Randeria, Phys. Rev. A **81**, 021601 (2010).
[16] E. Braaten, D. Kang, and L. Platter, Phys. Rev. Lett. **104**, 223004 (2010).
[17] In weak coupling $k_F|a_F| \ll 1$, the zero-temperature mean-field gap $\Delta/E_F = (8/e^2)\exp\{-\pi/(2k_F|a_F|)\}$ associated with long-range order is subleading with respect to Δ_∞ associated with medium-range order.
[18] P. Pieri and G. C. Strinati, Phys. Rev. Lett. **91**, 030401 (2003).
[19] E. D. Kuhnle *et al.*, e-print arXiv:1001.3200.
[20] The t-matrix approximation is extended to the superfluid case below T_c following P. Pieri, L. Pisani, and G. C. Strinati, Phys. Rev. B **70**, 094508 (2004).
[21] R. Combescot, S. Giorgini, and S. Stringari, Eur. Lett. **75**, 695 (2006).
[22] V. A. Belyakov, Sov. Phys. JETP **13**, 850 (1961).
[23] C. Chin and P. S. Julienne, Phys. Rev. A **71**, 012713 (2005).
[24] A. Perali, P. Pieri, and G. C. Strinati, Phys. Rev. Lett. **100**, 010402 (2008).
[25] The asymptotic behavior of transition matrix elements for large energy transfer depends on the short-range behavior of the two-body wave function [cf. A. R. P. Rau and U. Fano, Phys. Rev. **162**, 68 (1967)]. When final-state effects were taken into account, the rf signal would thus eventually acquire an $\omega^{-5/2}$ asymptotic tail [23,24].
[26] See supplementary material at [http://link.aps.org/supplemental/10.1103/PhysRevA.82.021605] for more details.
[27] H. Hu, X.-J. Liu, and P. D. Drummond, e-print arXiv:1003.3511.